Available online at www.sciencedirect.com
SCIENCE DIRECT®
Journal of Magnetic Resonance 172 (2005) 161–167
JMR Journal of Magnetic Resonance
www.elsevier.com/locate/jmr

Probing short length scales with restricted diffusion in a static gradient using the CPMG sequence

Lukasz J. Zielinski, Martin D. Hürlimann*

Schlumberger-Doll Research, 36 Old Quarry Road, Ridgefield, CT 06877-4108, USA

Received 25 August 2004

Abstract

We experimentally verify a new method of extracting the surface-to-volume ratio (S/V) of porous media with diffusion NMR. In contrast to the widely used pulsed field gradient (PFG) technique, which employs the stimulated echo coherence pathway, we use here the direct Carr–Purcell–Meiboom–Gill (CPMG) path. Even for high echoes, which exhibit ample attenuation due to diffusion in the field gradient, the relevant ruler length for the direct pathway is fixed by the diffusion length during a *single* inter-pulse spacing. The direct path, therefore, is well suited for probing shorter length scales than is possible with the conventional approach. In our experiments in a low-field static-gradient system, the direct CPMG pathway was found to be sensitive to structure an order of magnitude smaller than accessible with the stimulated-echo pathway.

Keywords: CPMG; Restricted diffusion; Inhomogeneous fields; Coherence pathways; Stray-field NMR; Constant gradient

1. Introduction

The pulsed field gradient (PFG) [1,2] diffusion measurement is a well-established NMR technique used to probe the structure of restricted geometries by tracking the motion of spins diffusing in the confined fluid [3]. It is especially useful in the study of systems with structure below the resolution of magnetic resonance imaging; and in the study of complex porous media, where the quantities of primary interest are the distributions of size and connectivity of pores.

The analysis of PFG measurements is usually based on the *narrow pulse approximation* [4–7] which requires, first of all, that the two phase-encoding gradient pulses be shorter than the spacing between them; and second, that the diffusion distance during the encoding time be short relative to the size of the structure of interest. In practice, these requirements imply that the shortest length scales accessible with the PFG technique are controlled by the strength and the switching rate of the available gradients.

One way to avoid the limitation of the gradient switching rate is to maintain a static gradient while using phase cycling to select the desired stimulated echo pathway [8]. The duration of the encoding period is then controlled by the radio-frequency (RF) pulses rather than the gradient pulses. A drawback of this method is that only the slice-selected region of the sample contributes to the signal. The requirement of a large gradient magnitude still remains, since the resulting diffusional attenuation has to be sufficient to be measured reliably. Consequently, with the moderate constant gradient of 13.17 G cm^{-1} used in our experiments, the stimulated-echo technique was only suitable to infer structure with length scales larger than 10 μm. This is illustrated in Fig. 1 which shows the time-dependent diffusion coefficient $D(t)$ for several samples with varying length scale of restriction. For short times, $D(t)$ is expected to fall

* Corresponding author.
E-mail addresses: hurlimann@slb.com, mhurlimann@ridgefield.oilfield.slb.com (M.D. Hürlimann).

1090-7807/$ - see front matter © 2004 Elsevier Inc. All rights reserved.
doi:10.1016/j.jmr.2004.10.006

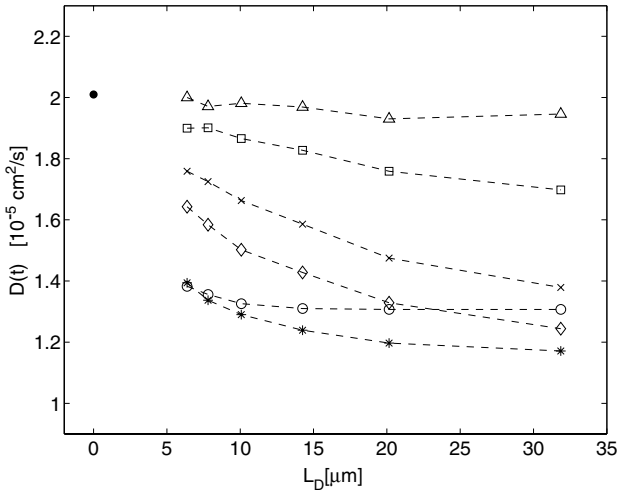

Fig. 1. Time-dependent diffusion coefficient extracted from the stimulated-echo measurements, plotted vs. the diffusion length $L_D = \sqrt{D_0 t}$, for bulk water, triangles; 160 μm sample, squares; 40 μm sample, exes; 16 μm sample, diamonds; 10 μm sample, asterisks; and 4 μm sample, circles. The bullet symbol marks $D_0 = 2.01 \times 10^{-5}$ cm^2 s^{-1} to which all the lines should extrapolate in the limit of $L_D = 0$.

off linearly with the diffusion length [9], with a slope proportional to the medium's surface-to-volume ratio (S/V)

$$D(t) = D_0\left[1 - \frac{4}{9\sqrt{\pi}}\frac{\sqrt{D_0 t}\,S}{V}\right]. \quad (1)$$

As is apparent from Fig. 1, only the 160 μm sample lies securely in the linear regime, while the 10 and 4 μm samples clearly are not. The diffusion length cannot be made any shorter without dramatically reducing the dynamic range of diffusive decay or violating the conditions of the narrow-pulse approximation, required for extracting $D(t)$. The first data point at $L_D = 6.4$ μm already is expected to exhibit a few-percent distortion due to the finite pulse width (see Eq. (19) in [7]).

An appealing approach to the problem of maintaining sensitivity to short length scales while ensuring sufficient diffusional attenuation is to use a sequence with a short segment repeated many times, such as the Carr–Purcell–Meiboom–Gill (CPMG) echo train in a static gradient or a sinusoidally oscillating gradient with a short period [10,11]. In terms of the spectral decomposition of the measured diffusion coefficient [12,3], either approach is suitable for examining the high-frequency (i.e., short-length-scale) range of the spectrum. No quantitative analysis of the effects of restriction on the spectrum has been given, however.

The purpose of the present paper is to experimentally explore the possibility of using the static-gradient CPMG to measure the S/V of porous media with structure on length scales shorter than attainable with the stimulated echo technique. In reference to Fig. 1, this goal translates to filling in the inaccessible short-L_D points in the linear region where the short-time theory that yields the S/V applies. In the presence of a constant gradient and, consequently, slice selective RF pulses, many coherence pathways are excited, even by the simple CPMG pulse train. The pathway of interest here is the direct-echo pathway that contributes to the CPMG echoes on resonance. It is this pathway that has the promising characteristics that make it a good candidate for probing short length scales.

First of all, as we have recently confirmed experimentally [13], the relevant diffusion time for the direct path is fixed by the spacing between two *adjacent* echoes, regardless of the duration of the entire pulse train. And second, already for the first (Hahn) echo, the CPMG in a static field maximizes the diffusional attenuation for the given diffusion time, which is what sets the lower bound on the length scale probed. The amount of attenuation further increases with echo number, while the ruler length remains fixed by a *single* inter-pulse spacing. Thus, in principle at least, one should be able to reach very short length scales by keeping the pulse spacing short and looking at high echoes to get sufficient dynamic range to extract diffusional relaxation. Another welcome feature of the CPMG is that it is already widely used in many stray-field applications due to its superior signal-to-noise characteristics important in low fields. Incorporating the effects of restriction into the analysis of such pulse trains could yield useful additional information.

We focus on the short-time diffusion regime, where the spins accumulate little phase while diffusing in the gradient and traverse distances shorter than the size of the geometrical structure of the confining medium. In this regime, as for the PFG-measured time-dependent diffusion coefficient in Eq. (1), the correction to the unrestricted-fluid behavior is proportional to the surface-to-volume (S/V) ratio of the pore space. If D_0 is the diffusion coefficient of the bulk fluid, g a uniform static gradient, γ is the proton gyromagnetic ratio, and τ is half the echo spacing, then, provided the RF pulses are applied on resonance, the attenuation of the direct pathway at the nth CPMG echo can be written as

$$M_{n,\tau} = M_0 R(2n\tau) \times \exp\left\{-\frac{2n}{3}\gamma^2 g^2 \tau^3 D_0\left(1 + \frac{C(n)}{6n}\frac{S\sqrt{D_0\tau}}{V}\right)\right\}, \quad (2)$$

where $R(2n\tau)$ gives the T_2 relaxation and $C(n)$ are negative numerical coefficients that can be computed analytically and have been tabulated in [14]. This result was first derived by Axelrod and Sen [15] and then extended to arbitrary coherence pathways, finite surface relaxation, and strongly inhomogeneous fields in [16–18]. The general theory was experimentally verified in [13]. Here, we investigate in more detail its implications for the direct CPMG pathway, which, as already

mentioned, remains in the short-time regime even when the duration of the entire pulse train is long. We experimentally demonstrate that the CPMG sequence allows us to reach length scales an order of magnitude shorter than attainable with the stimulated echo measurement on the same system.

2. Experimental details

We performed measurements on several brine-saturated fused-glass cylindrical plugs from RobuGlas,[1] with 2 cm diameter and 2 cm height and pore sizes ranging from ~4 to ~250 μm. The five materials used were already characterized in [13], where the surface-to-volume ratios, measured both with NMR and with BET gas-adsorption, as well as manufacturer's listed throat size ranges, were reported in Table 2. We will adhere to the naming convention adopted in [13] and refer to each sample by its lower cut-off throat size, as given by the manufacturer. Thus, we have the 160, 40, 16, 10, and 4 μm sample.

The samples were placed in the fringe field of a superconducting magnet in a static gradient of 13.17 G cm^{-1} perpendicular to the cylinder axis, with the center Larmor frequency of 1.764 MHz. The quality factor of the receiver was $Q = 13.4$, and the 180° pulses were 24 μs long. We collected entire echo shapes, with the dwell time of 8 μs and 32 acquisition points per echo. The samples were temperature controlled at 22 °C to eliminate fluctuations in the bulk fluid diffusion coefficient, which we measured to be $D_0 = 2.01 \pm 0.02 \times 10^{-5}$ cm^2 s^{-1}, in good agreement with the literature values.

We applied the usual CPMG sequence [19,20] 90°–τ–180°–2τ–180°–2τ–$\cdots$, with the spacing between the initial 90° pulse and the first 180° reduced by $t_1 = \omega_1^{-1}$ to optimize signal-to-noise in the presence of field inhomogeneity [21]. Since $t_1 \ll \tau$, for the purposes of computing diffusional attenuation, this adjustment can be ignored. We varied the echo spacing 2τ and collected 100 echoes for each value of τ, thus acquiring a two-dimensional data set for each sample, that maps out the n and τ dimensions in Eq. (2). The on-resonance echo amplitudes, $M_{n,\tau}$, were extracted by integrating the entire echo shape. This is equivalent to applying a step window function with a bandwidth of 3.9 kHz, which is 0.2 of the width of the excited slice ($\omega_1 = 2\pi \times 21$ kHz). For such a narrow bandwidth, most of the contribution to the signal will come from the direct pathway [22], even for high echoes. Furthermore, the only other coherence pathways that will begin to contribute to the signal after multiple 180° pulses will have diffusional properties very similar to the direct path [23]. They should not, therefore, significantly affect the measured diffusion coefficient or S/V ratio, as we have explicitly verified by numerical simulations of our system, that included all the coherence pathways. The ultimate proof that this procedure does, in fact, correctly extract the on-resonance (and, thus, the direct-pathway) contribution lies in the bulk-water data (see Section 3.1) that shows no deviations from the well-understood diffusion-in-uniform-gradient theory.

To extract the diffusional attenuation in Eq. (2), we first calibrated the T_2 relaxation term $R(2n\tau)$ for each sample with an independent CPMG measurement of 8000 echoes with a short echo spacing $2\tau = 424$ μs. We found the relaxation to be single exponential (see Fig. 2), allowing us to express it, for each sample, as $R(2n\tau) = \exp\{-2n\tau/T_2\}$, with an appropriate T_2 decay time constant. The echo amplitudes for the T_2 measurement were extracted by optimal filtering with the asymptotic echo shape [24]. As discussed in detail in [22,25], in systems with grossly inhomogeneous fields (i.e., weak RF field), such procedure yields an effective T_2 that is a mixture of T_1 (due to non-direct pathways), of $T_{1\rho}$ (due to relaxation while the RF field is on), and of the actual T_2. In our experiments, this introduces an uncertainty of up to ~5% in the actual T_2, with the effective T_2 providing an upper bound. Nonetheless, throughout, we will use the measured effective T_2's as if they were the ground-truth T_2's and point out where the uncertainty bears on the discussion of the two-dimensional CPMG measurements that are the main focus of the present work.

Lastly, the stimulated-echo experiments were carried out in the same fringe-field set-up, following the prescription provided for the diffusion-editing sequence in

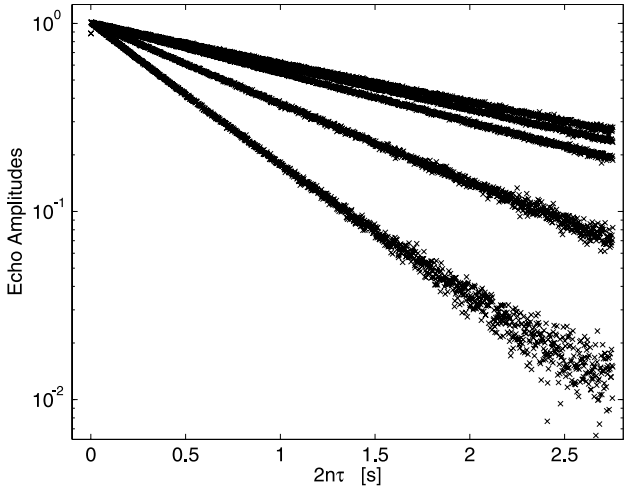

Fig. 2. CPMG measurement of T_2, with echo spacing $2\tau = 424$ μs, for the five samples used, plotting every fifth echo. From top to bottom: 160 μm sample, $T_2 = 2.15$ s; 40 μm sample, $T_2 = 1.90$ s; 16 μm sample, $T_2 = 1.65$ s; 10 μm sample, $T_2 = 1.02$ s; and 4 μm sample, $T_2 = 0.565$ s. All curves exhibit single-exponential behavior.

[1] http://www.robu.net.

[8]. The initial 90° pulse was followed by another one applied at time δ and the third one at time Δ. Sixteen-stage phase cycling was performed to select out the stimulated pathway. The echo then formed at time $t = \Delta + \delta$, defining the relevant diffusion length via $\sqrt{D_0 t}$ (see Fig. 1). Finally, a train of 300 narrowly spaced ($2\tau = 424$ μs) 180° pulses was applied for each δ–Δ pair and the acquired echoes summed for improved signal-to-noise ratio.

3. Results

3.1. Unrestricted diffusion: bulk brine

We calibrated our experimental procedure by first performing the two-dimensional CPMG experiment on a bulk water sample, having the same dimensions as the RobuGlas plugs, doped with NiCl to give $T_1 = 642$ ms and $T_2 = 602$ ms. Noting that for the longest echo spacings the signal decays already after a few echoes, we modified the usual least-squares fitting procedure in order to balance the contributions of short and long τ's. For each τ, we weighted the cost function inversely with the number of echoes, for that τ, with amplitude above noise level. Without this amendment, the fits were heavily dominated by the short-τ data and, thus, artificially oversensitive to T_2 relaxation at the expense of decay due to diffusion in the gradient. Using the weighted cost function, on the other hand, produced very stable fits. Whether T_2 was fixed at $T_2 = 602$ ms or whether it was treated as a free parameter alongside the diffusion coefficient, the fitted value for D_0 was unchanged at $D_0 = 2.01 \times 10^{-5}\,\mathrm{cm^2\,s^{-1}}$, in excellent agreement with the value independently measured with a stimulated-echo experiment. Similarly, treating M_0 as another fitting parameter or else extracting it only from the shortest-τ data and using that value as fixed in the two-dimensional fit, did not affect the value obtained for D_0. Fig. 3 shows the agreement of the data with the bulk theory.

In Figs. 4A and B we show that every one of the lines in of Fig. 3 can be used to independently extract D_0. Thus, assuming $T_2 = 602$ ms, for each echo individually one can fit D_0 from Eq. (2) along the τ^3 dimension (setting $S/V \to 0$ as is appropriate for bulk fluid). The results of such procedure are shown in Fig. 4A. Similarly, for each value of τ, one can fit D_0 along the echo dimension, as shown in Fig. 4B. The D_0 points extracted from the shortest echo spacings, corresponding to $\sqrt{D_0\tau} < 1.6$ μm, were very sensitive to the precise value of T_2. And while it was possible to tweak the T_2 by a few percent to make them fall on the $D_0 = 2.01 \times 10^{-5}\,\mathrm{cm^2\,s^{-1}}$ line, which could well be justified given the uncertainty in T_2 discussed in Section 1, we chose not to display these data.

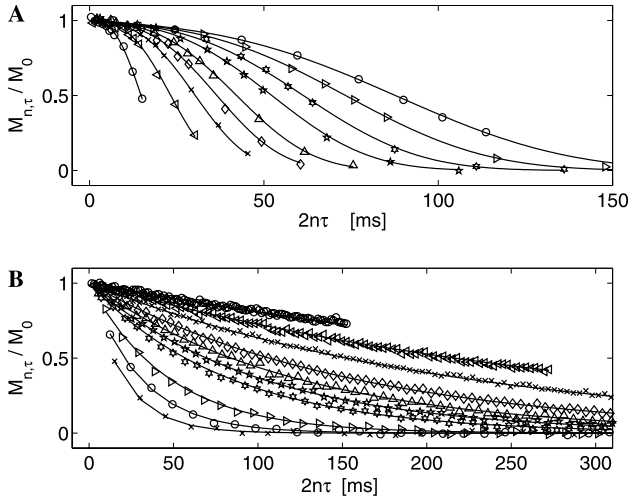

Fig. 3. CPMG measurement on bulk water; for each of the 10 different values of the echo spacing 2τ, 100 echoes were collected. We plot the normalized echo amplitudes $M_{n,\tau}$ (markers), and the bulk-fluid theory (solid lines), using $D_0 = 2.01 \times 10^{-5}\,\mathrm{cm^2\,s^{-1}}$ and $T_2 = 0.604$ s. (A) Each marker style and each line follows a single echo for all values of τ; from left to right, echoes 1, 2, …, 5, 7, 9, 12, and 16. (B) Each marker style and each line follows a single τ starting with the first echo; from top to bottom, $\tau = 0.762$, 1.362, 1.862, 2.412, 2.812, 3.162, 3.552, 4.862, 6.162, and 7.562 ms.

3.2. Restricted diffusion: sintered-glass samples

We followed a similar fitting strategy for the restricted samples, but now fixing $D_0 = 2.01 \times 10^{-5}\ \mathrm{cm^2\,s^{-1}}$ and extracting the V/S term in Eq. (2). As for bulk water, we weighted the data for each value of τ in the least-squares cost function according to the number of echoes

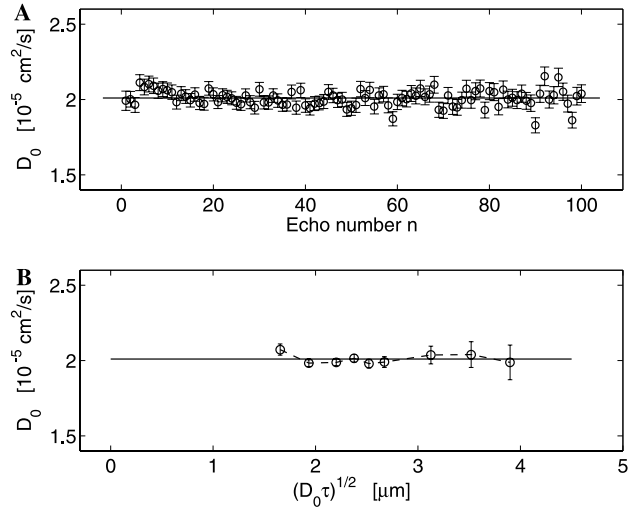

Fig. 4. Extracted diffusion coefficient from the CPMG measurement on bulk water (same data set as shown in Fig. 3): (A) fits of D_0 from individual echoes (with τ^3 as the variable); and (B) fits of D_0 from individual τ values (with the echo number as the variable). Solid lines indicate $D_0 = 2.01 \times 10^{-5}\,\mathrm{cm^2\,s^{-1}}$. T_2 decay was divided out prior to all fitting, using the independently measured $T_2 = 0.604$ s. Error bars derive from random noise in the out-of-phase channel.

for that τ with amplitudes above noise level. Fig. 5 shows the results of such a weighted fit for the 16 μm sample. Both D_0 and T_2 were held fixed; V/S and M_0 were the only free parameters. The agreement between the experiment and the short-time theory is excellent and was equally good for the other RobuGlas samples.

The fits of the surface-to-volume ratio for the various samples proved quite robust with respect to small changes in the parameter values. For instance, fixing T_2 at the independently measured values (Fig. 2) or using values shorter by 15% or letting T_2 be a free parameter did not affect the extracted V/S by more than a few percent. Varying D_0 within the uncertainty interval ($\pm 0.02 \times 10^{-5}$ cm^2 s^{-1}) had little effect on the V/S of small samples (a few percent) but more on the larger samples (up to 50% for the 160 μm sample). This is not surprising since the technique is not well suited for studying long length scales, for which the S/V correction in Eq. (2) at the attainable diffusion lengths is quite small (see Section 4). But even for the 160 μm sample, the V/S extracted from the two-dimensional fit, assuming $D_0 = 2.01 \times 10^{-5}$ cm^2 s^{-1}, was 35 μm, in excellent agreement with the stimulated-echo data (see Fig. 6B).

To compare more directly the length scales probed with our CPMG technique with those probed by the stimulated echo, we follow [13], where the relevant diffusion length was defined for arbitrary coherence pathways. For the nth CPMG echo direct pathway, the relevant diffusion length will be given by

$$L_{n,\tau} \equiv -(9\sqrt{\pi}/4)(C(n)/6n)\sqrt{D_0\tau}, \tag{3}$$

whereby Eq. (2) assumes a form similar to Eq. (1)

$$M_{n,\tau} = M_0\, R(2n\tau) \times \exp\left\{-\frac{2n}{3}\gamma^2 g^2 \tau^3 D_0\left(1 - \frac{4}{9\sqrt{\pi}}\frac{L_{n,\tau}S}{V}\right)\right\}. \tag{4}$$

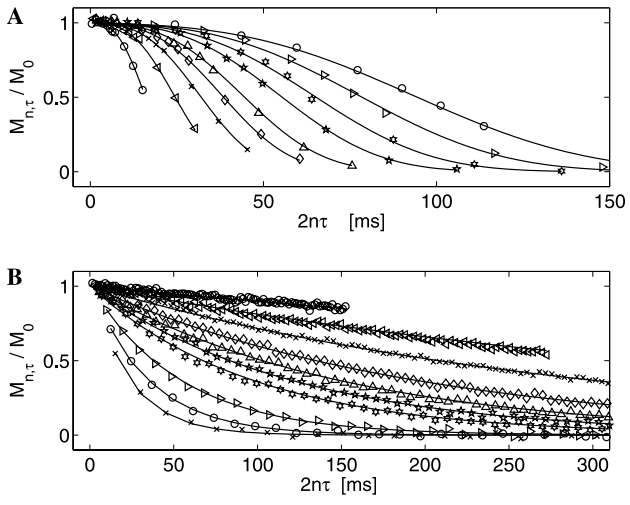

Fig. 5. Normalized echo amplitudes $M_{n,\tau}$, markers, in the same order as in Fig. 3, for the 16 μm sample. Solid lines give the short-time theory, Eq. (2), with $V/S = 6.5$ μm fit from the entire data set, assuming $D_0 = 2.01 \times 10^{-5}$ cm^2 s^{-1} and independently measured $T_2 = 1.65$ s.

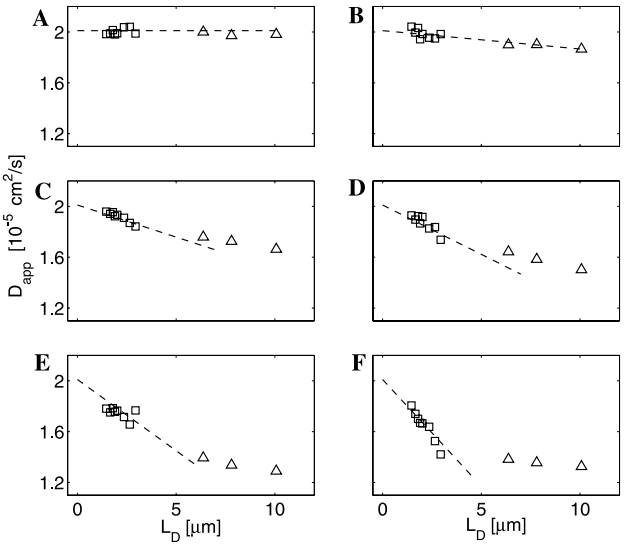

Fig. 6. The apparent CPMG diffusion coefficient, Eq. (6), squares, plotted vs. $L_D = L_{CPMG} \approx 0.76\sqrt{D_0\tau}$; and the stimulated-echo time-dependent diffusion coefficient, Eq. (1), triangles, plotted vs. $L_D = \sqrt{D_0 t}$. The stimulated-echo data are the same as shown in Fig. 1 (first three points). (A) Bulk water; (B) 160 μm sample, $V/S = 35$ μm; (C) 40 μm sample, $V/S = 10$ μm; (D) 16 μm sample, $V/S = 6.5$ μm; (E) 10 μm sample, $V/S = 4.5$ μm; and (F) 4 μm sample, $V/S = 3$ μm. The V/S quoted were obtained from weighted two-dimensional fits to the entire data sets as described in the text. The dashed lines give D_{app} from Eq. (6) plotted with the appropriate V/S.

Now we note that the $C(n)$ coefficients reach an asymptotic limit, $C(n)/6n \to 0.19$, already after several echoes. Thus, up to some oscillations in the early echoes, which are of the order of the experimental uncertainties, one can define a unique CPMG length scale

$$L_{CPMG} \equiv \lim_{n\to\infty} L_{n,\tau} \approx 0.76\sqrt{D_0\tau}, \tag{5}$$

which is independent of echo number. Then one can also define an apparent CPMG diffusion coefficient

$$D_{app} = D_0\left[1 - \frac{4}{9\sqrt{\pi}}\frac{L_{CPMG}\,S}{V}\right]. \tag{6}$$

L_{CPMG} gives the relevant length scale probed with a CPMG train with echo spacing 2τ. It plays a role analogous to $\sqrt{D_0 t}$ in the stimulated-echo measurement of the time-dependent diffusion coefficient $D(t)$ in Eq. (1).

Experimentally, D_{app} was extracted from the data in the same way as D_0 in Fig. 4B. First, T_2 relaxation $R(2n\tau)$ was divided out using the appropriate T_2 from Fig. 2. Next, for each value of τ, a fit to $\exp\{-(2n/3)\gamma^2 g^2 \tau^3 D_{app}\}$ was performed down to noise level along the echo dimension. The results for bulk water and the five RobuGlas samples are shown in Fig. 6. The values of D_{app} extracted from the CPMG sequence, plotted vs. $L_D = L_{CPMG}$ are shown as squares, while the triangles mark the first three data points from the stimulated echo measurement of $D(t)$ in Fig. 1 plotted vs. $L_D = \sqrt{D_0 t}$. The dashed lines indicate the slopes with

V/S extracted from two-dimensional CPMG fits as described above. Apparently, the CPMG based D_{app} measurements lie in the linear regime with respect to L_{CPMG} and so Eq. (6) is appropriate. Thus, the CPMG can indeed be used to fill in the short-length-scale data that were amiss in Fig. 1.

4. Discussion

While it is possible to treat the apparent CPMG diffusion coefficient just as the $D(t)$ from a PFG measurement and, in analogy, as suggested by Fig. 6, fit V/S from the slope of D_{app} vs. L_{CPMG}, this is not the preferred method. By collapsing the echo dimension, one throws away the bulk of information, resulting in a rather noisy line. Unlike in the PFG experiment, where $D(t)$ is the fundamental computed quantity that is to be measured, here every (n,τ) point in the data set contains the same information given by Eq. (2). The quantity we are after is the surface-to-volume ratio of the medium, and that is best extracted by performing a full two-dimensional fit to the entire data set, as described earlier. Defining D_{app} and plotting it alongside the PFG-measured time-dependent diffusion coefficient is a useful exercise, however, as it more concretely illustrates the regimes in which the two techniques apply.

The direct CPMG pathway will not be useful for probing length scales longer than the *dephasing length*, $L_G = (D_0/\gamma g)^{1/3}$, which is the typical distance a spin must diffuse before acquiring a phase of $\sim 2\pi$. The reason is twofold. First of all, since $\gamma^2 g^2 \tau^3 D_0 = (L_D/L_G)^6$, where $L_D = \sqrt{D_0 \tau}$, the signal will attenuate very rapidly when the diffusion length L_D becomes longer than L_G (see Eq. (2)). On the other hand, if L_D remains much shorter than L_G, then very few spins will feel the presence of the walls and, hence, the $L_D S/V$ correction will be difficult to detect. This issue is apparent in Fig. 6B. In our system, $L_G = 3.85$ μm, setting the bound on the longest L_D that can be used. For the 160 μm sample, $V/S = 35$ μm, and so $(4/9\sqrt{\pi})\, L_D\, S/V \sim 0.03$, hardly allowing sufficient dynamic range for a reliable measurement.

The stimulated pathway, on the other hand, is ideally suited for probing long length scales because it is controlled by two different times, the encoding time δ and the diffusion time Δ. Only $\sqrt{D_0 \delta}$ must be shorter than L_G in order to be in the right regime [7]; $\sqrt{D_0 \Delta}$ can be long, making the measurement sensitive to larger structure.

When the structure of interest is of the order of the dephasing length, then the direct CPMG pathway is preferable for reaching the short-time regime given in Eqs. (1) and (2). In our case, already the 40 μm sample, with $V/S = 10$ μm, falls into this category. As is apparent from Fig. 1 ('x' markers), the stimulated pathway for this sample has not yet fully reached the regime linear in L_D; linear extrapolation to $L_D = 0$ from the last three points would underestimate the D_0 and overestimate V/S. The corresponding direct pathway, on the other hand, as shown in Fig. 6C, gives a sensible slope through the correct value of $D_0 = 2.01 \times 10^{-5}\ \mathrm{cm^2\ s^{-1}}$. For the two smallest samples, 10 and 4 μm, the stimulated pathway can yield hardly any information about their V/S, while the direct path gives consistent results.

Thus, when characterizing a new material, it is probably best to start with a PFG sequence, to obtain the $D(t)$ for a large range of length scales, and then complement it with the CPMG technique, if there is apparent smaller structure that needs to be studied more carefully.

5. Conclusion

We have experimentally validated a new method for extracting the surface-to-volume ratio of porous media with diffusion NMR. This CPMG-based technique allows probing smaller structure than is possible with the conventional stimulated echo pulsed field gradient method. It relies on the fact that the relevant diffusion length for the direct CPMG pathway remains fixed by the spacing between two adjacent 180° pulses, even for high echo numbers. Since the amount of attenuation increases with echo number, one can obtain sizable dynamic range even for very short diffusion lengths. The new CPMG technique complements the PFG in the characterization of heterogeneous media, as the conventional method is superior for probing larger structure.

The lower bound on length scales accessible with the CPMG is set, fundamentally, by the T_1 and T_2 relaxation. Since the diffusional attenuation falls off as $n\tau^3$ while the surface relaxation only as $n\tau$, as shorter pulse spacings are used in order to reach shorter length scales, eventually, surface relaxation will dominate and render the measurement of diffusional attenuation unreliable. This limitation is not specific to the proposed CPMG technique, however, but applies to any NMR diffusion measurement.

Acknowledgments

The authors are grateful for useful discussions with Edmund J. Fordham and Pabitra N. Sen.

References

[1] E.O. Stejskal, J.E. Tanner, Spin diffusion measurements: spin echoes in the presence of a time-dependent field gradient, J. Chem. Phys. 42 (1965) 288.
[2] J.E. Tanner, Use of the stimulated echo in NMR diffusion studies, J. Chem. Phys. 52 (5) (1970) 2523.
[3] P.T. Callaghan, Principles of Nuclear Magnetic Resonance Microscopy, Oxford University Press, New York, 1993.

[4] L.Z. Wang, A. Caprihan, E. Fukushima, The narrow-pulse criterion for pulsed-gradient spin-echo diffusion measurements, J. Magn. Reson. Ser. A 117 (1995) 209–219.
[5] P.P. Mitra, B.I. Halperin, Effects of finite gradient-pulse widths in pulsed-field-gradient diffusion measurements, J. Magn. Reson. Ser. A 113 (1995) 94.
[6] R.W. Mair, P.N. Sen, M.D. Hürlimann, S. Patz, D.G. Cory, R.L. Walsworth, Narrow pulse approximation and long length scale determination in xenon gas diffusion NMR studies of model porous media, J. Magn. Reson. 156 (2002) 202.
[7] L.J. Zielinski, P.N. Sen, Effects of finite-width pulses in the pulsed-field gradient measurement of the diffusion coefficient in connected porous media, J. Magn. Reson. 165 (2003) 153–161.
[8] M.D. Hürlimann, L. Venkataramanan, Quantitative measurement of two-dimensional distribution functions of diffusion and relaxation in grossly inhomogeneous fields, J. Magn. Reson. 157 (2002) 31–42.
[9] P.P. Mitra, P.N. Sen, L.M. Schwartz, Short-time behavior of the diffusion coefficient as a geometrical probe of porous media, Phys. Rev. B 47 (1993) 8565.
[10] J. Stepišnik, Analysis of NMR self-diffusion measurements by a density matrix calculation, Physica 104B (1981) 350–364.
[11] B. Gross, R. Kosfeld, Anwendung der Spin-Echo-Methode bei der Messung der Selbstdiffusion, Messtechnik 7/9 (1969) 171.
[12] J. Stepišnik, Measuring and imaging of flow by NMR, Prog. NMR Spectr. 17 (1985) 187–209.
[13] L.J. Zielinski, M.D. Hürlimann, Short-time restricted diffusion in a static gradient and the attenuation of individual coherence pathways, J. Magn. Reson. 171 (2004) 107–117.
[14] P.N. Sen, A. André, S. Axelrod, Spin echoes of nuclear magnetization diffusing in a constant magnetic field gradient and in a restricted geometry, J. Chem. Phys. 111 (1999) 6548.
[15] S. Axelrod, P.N. Sen, Nuclear magnetic resonance spin echoes for restricted diffusion in an inhomogeneous field: methods and asymptotic regimes, J. Chem. Phys. 114 (2001) 6878.
[16] L.J. Zielinski, P.N. Sen, Combined effects of diffusion, nonuniform-gradient magnetic fields, and restriction on an arbitrary coherence pathway, J. Chem. Phys. 119 (2003) 1093.
[17] L.J. Zielinski, P.N. Sen, Restricted diffusion in grossly inhomogeneous fields, J. Magn. Reson. 164 (2003) 145–153.
[18] L.J. Zielinski, Effect of internal gradients in the nuclear magnetic resonance measurement of the surface-to-volume ratio, J. Chem. Phys. 121 (2004) 352–361.
[19] H.Y. Carr, E.M. Purcell, Effects of diffusion on free precession in NMR experiments, Phys. Rev. 94 (1954) 630.
[20] S. Meiboom, D. Gill, Compensation for pulse imperfections in Carr–Purcell NMR experiments, Rev. Sci. Instrum. 29 (1958) 688.
[21] M.D. Hürlimann, Optimization of timing in the Carr–Purcell–Meiboom–Gill sequence, Magn. Reson. Imag. 19 (2001) 375–378.
[22] G. Goelman, M. Prammer, The CPMG pulse sequence in strong magnetic field gradients with applications to oil-well logging, J. Magn. Reson. Ser. A 113 (1995) 11–18.
[23] Y.-Q. Song, Categories of coherences for the CPMG sequence, J. Magn. Reson. 157 (2002) 82–91.
[24] M.D. Hürlimann, Diffusion and relaxation effects in general stray field NMR experiments, J. Magn. Reson. 148 (2001) 367–378.
[25] M.D. Hürlimann, D.D. Griffin, Spin dynamics of Carr–Purcell–Meiboom–Gill-like sequences in grossly inhomogeneous B_0 and B_1 fields and application to NMR well logging, J. Magn. Reson. 143 (2000) 120–135.